ATLAS Internal Note
PHYS-NO-060
12 Janvier 1995

Gauge bosons pairs production study with Atlas

Dominique Fouchez
Centre de Physique des Particules de Marseille
13288 Marseille,France

Abstract

The possibility to detect anomalous couplings in the gauge boson sector is investigated in the context of the ATLAS detector at LHC. The measurements of distributions of kinematic variables from gauge bosons pair production allows a measurement of possible anomalous couplings for both WWZ and $WW\gamma$ vertices or to set limits on them. For this study the main sources of background with leptons and photons are considered and appropriate cuts to minimize them are applied.

1 Introduction

There is a strong interest to study the couplings between gauge bosons : the coupling of three gauge bosons, which is fixed by the SU(2) symmetry of the Standard Model can exhibit underlying non-standard physics. Indeed many kinds of new physics give non-standard contributions to this particular vertex [1] [2] and measurements of possible anomalous couplings may offer a way to reach the origin and structure of the Higgs sector [3].

In the Standard Model, the three boson vertices come from the non-commutative part of the SU(2)$\otimes$U(1) gauge symmetry. The Lagrangian of the free field (when restricting ourselves to SU(2)) is written as :

$$\mathcal{L} = -\frac{1}{4}\, W_i{}^{\mu\nu} W_{i\,\mu\nu}$$

with $W_i{}^{\mu\nu} = \partial^\mu W_i{}^\nu - \partial^\nu W_i{}^\mu + g\epsilon_{ijk} W_j{}^\mu W_k{}^\nu \;\;, \qquad (i = 1,2,3)$

The $g\epsilon_{ijk} W_j{}^\mu W_k{}^\nu$ term will generate, in the perturbative development, the following graphs, which are respectively the three boson and four boson vertices:

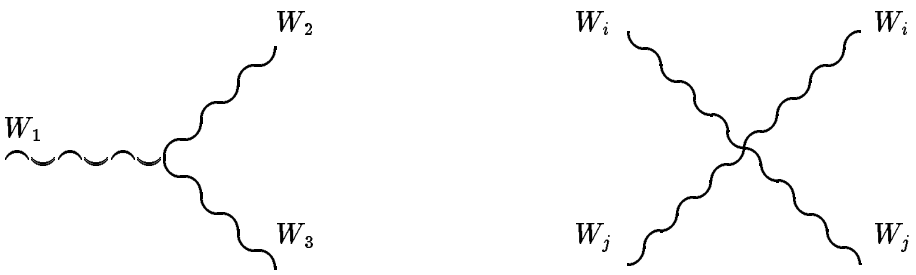


Figure 1: Three and four bosons graphs of the electroweak Standard Model

If some non-standard physics appears, the Lagrangian of the Standard Model can be replaced by an effective Lagrangian written, if terms violating discrete symmetries (C,P,CP) are not taken into account, as:

a) for the $WW\gamma$ case:

$$\mathcal{L}_{WW\gamma} = -ie\left\{(W^\dagger_{\mu\nu} W^\mu A^\nu - W^\dagger_\mu A_\nu W^{\mu\nu}) + \kappa_\gamma W^\dagger_\mu W_\nu F^{\mu\nu} + \frac{\lambda_\gamma}{m_W^2} W^\dagger_{\alpha\mu} W^\mu_\nu F^{\nu\alpha}\right\},$$

where A^μ and W^μ are respectively the photon and W fields and
$W_{\mu\nu} = \partial_\mu W_\nu - \partial_\nu W_\mu$, $F_{\mu\nu} = \partial_\mu A_\nu - \partial_\nu A_\mu$ et $\tilde{F}_{\mu\nu} = \frac{1}{2}\epsilon_{\mu\nu\rho\sigma} F^{\rho\sigma}$.

b) for the WWZ case :

$$\mathcal{L}_{WWZ} = -ie\, cot\theta_W \left\{g_1(W^\dagger_{\mu\nu} W^\mu Z^\nu - W^\dagger_\mu Z_\nu W^{\mu\nu}) + \kappa_Z W^\dagger_\mu W_\nu Z^{\mu\nu} + \frac{\lambda_Z}{m_W^2} W^\dagger_{\alpha\mu} W^\mu_\nu Z^{\nu\alpha}\right\},$$

where Z^μ and W^μ are respectively the Z and W fields and
$W_{\mu\nu} = \partial_\mu W_\nu - \partial_\nu W_\mu$, $Z_{\mu\nu} = \partial_\mu Z_\nu - \partial_\nu Z_\mu$ et $\tilde{Z}_{\mu\nu} = \frac{1}{2}\epsilon_{\mu\nu\rho\sigma} Z^{\rho\sigma}$.

We will, in addition, fix here g_1 =1, i.e. its Standard Model value, to restrict the study to pure three boson vertex anomalies.

We have then a set of 4 parameters that can describe, in a "general way" possible non-standard physics (in the Standard Model : κ_γ=1, λ_γ=0, κ_Z=1, λ_Z=0). The present bounds on those parameters are of several hundred % and are expected to be reduce at the level of 10% at LEP 200.

Another important point for the relevance of the study concerning the three boson vertices at high energy is the form factor. In compositeness model it is usual to include a form factor, wich describes the spatial extension of the proton charge :

$$F_\Lambda(\hat{s}) = \frac{1}{(1+\frac{\hat{s}}{\Lambda^2})^n},$$

where Λ is associated to the "size" of the system [4] [2] and can be identified with the energy scale where compositeness manifests itself.

This form factor is necessary here because of the process: $e^+e^- \rightarrow W^+W^-$, which restricts the $WW\gamma$ coupling to its Standard Model value for asymptotically high energy (this is also true for the WWZ vertex).

2 The signals

In hadron colliders like the LHC, the three boson vertices ($WW\gamma$ and WWZ) take part in gauge boson pair production (i.e. $W\gamma$, WZ and W^+W^-).

The two processes studied in this note are the production of $W\gamma$ and WZ. The W^+W^- process is swamped by $t\bar{t}$ background, two orders of magnitude higher.

The production of a gauge boson pair in a hadron collider involves the three following graphs:

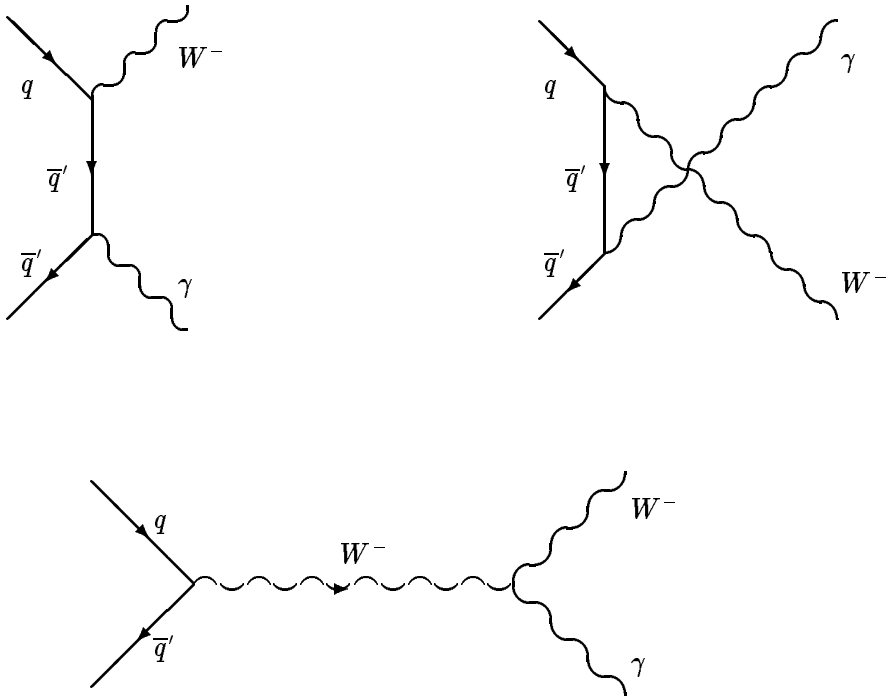


Figure 2: Diagrams for boson pair production

A possible abnormal contribution to $W\gamma$ production $\Delta\mathcal{M}_{h_\gamma h_W}$ (where h_W and h_γ are the W and γ helicities) can be written as [8] :

$$\Delta\mathcal{M}_{\pm\, o} = \frac{e^2}{\sin\theta_W}\,\frac{\sqrt{\hat{s}}}{2m_W}\,[\kappa_\gamma - 1 + \lambda_\gamma]\frac{1}{2}(1 \mp \cos\Theta)$$

and

$$\Delta\mathcal{M}_{\pm\pm} = \frac{e^2}{\sin\theta_W}\,\frac{\hat{s}}{2m_W^2}\,\lambda_\gamma\,\frac{1}{\sqrt{2}}\sin\Theta$$

where Θ is the scattering angle of the photon with respect to the quark direction.

These contributions increase to infinity at high energy and this demonstrates the need for a fom factor. We can also conclude that deviations from the Standard Model will increase with energy.

The signal for possible non-standard couplings will appear in the invariant mass of the gauge boson pair where an excess of events compared to the Standard Model is expected at the highest energies (e.g. in transverse momentum and transverse mass distribution). For the $W\gamma$ case, non-standard couplings can also be searched for in the angular distribution of the photon where a zero amplitude is expected in the Standard Model, for a particular value of this angle.

The signal processes have to use leptonic decays of the W and Z, so that they can be triggered on and also that they are not swamped by purely hadronic events from QCD production.

3 The simulation of the detector and event generation

The simulation of the detector is done in the following way, using simple parametrisation of the ATLAS performance :

a) The electromagnetic calorimeter is divided into projective cells with a granularity $\Delta\eta \times \Delta\phi = 0.02 \times 0.02$ and with a rapidity $|\eta| < 3$. For electrons and photons, all the energy of the particle is deposited in the hit cell with a smearing according to the following resolution:

$$\frac{\sigma}{E} = \left(\frac{a}{\sqrt{E}} \oplus b \oplus \frac{c}{\sqrt{E}}\right)\alpha_{crack} \oplus \frac{d}{E},$$

where

$a = 0.10$	Sampling term
$b = 0.007$	Constant term
$c = 0.02$	Term to take into account material in front of the calorimeter
$d = 0.250$	Electronic noise term
$\alpha_{crack} = \begin{cases} 4, & \text{if } 1.74 < \lvert\eta\rvert < 1.86; \\ 1, & \text{if not.} \end{cases}$	Factor to simulate energy degradation in the crack region between barrel and end-caps.

b) For the hadronic part, the granularity is twice coarser and the resolution is given by :

$$\frac{\sigma}{E} = \left(\frac{a}{\sqrt{E}} \oplus b\right) \alpha_{crack},$$

where

$a = 0.50$	Sampling term
$b = 0.02$	Constant term
$\alpha_{crack} = \begin{cases} 4, & \text{if } 1.74 < \lvert\eta\rvert < 1.86; \\ 1, & \text{if not.} \end{cases}$	Factor to simulate energy degradation in the crack region between barel and end-caps.

c) For the muons, the momentum is smeared according to the parametrisation of the Atlas muon spectrometer up to $|\eta| < 3$ [5].

d) For this study the p_T threshold (i.e. the trigger requirements) for photons, electrons and muons is above 20 GeV, with a rapidity coverage up to $|\eta|$=2.5

e) A classical jet algorithm (UA1-like) is used to reconstruct the jets.

The event generation used PYTHIA 5.7. The centre-of-mass energy is $\sqrt{s}$= 14 TeV, with an integrated luminosity of 10^5 pb^{-1} per year. For the standard processes, the PYTHIA matrix elements were used, except for $Zb\bar{b}$ and anomalous couplings that have been introduced into PYTHIA from matrix element calculations as external processes.

4 Study of $W\gamma$ production

We restrict this study to the leptonic decay of the W. The trigger is then defined as two electromagnetic clusters (γe) ore one electromagnetic cluster and a muon ($\gamma \mu$), all of high p_T.

The background comes from processes with a γ and a lepton in the final state :

- Real γ and real lepton:

  $pp \rightarrow \gamma b\bar{b}\ (+X) \rightarrow \gamma l\nu\ (+X)$
  $pp \rightarrow \gamma t\bar{t}\ (+X) \rightarrow \gamma l\nu\ (+X)$
  $pp \rightarrow \gamma Z\ (+X) \rightarrow \gamma ll\ (+X)$

- Real γ and fake electron (no fake muons of high-p_T are expected in ATLAS):

  $pp \rightarrow \gamma + jet\ (+X)$

- Fake γ and real lepton:

  $pp \rightarrow W + jet\ (+X) \rightarrow l\nu + jet\ (+X)$
  $pp \rightarrow b\bar{b}\ (+X) \rightarrow l\nu + jet\ (+X)$
  $pp \rightarrow t\bar{t}\ (+X) \rightarrow l\nu + jet\ (+X)$

We summarise in Table 1 the relative importance of the various backgrounds using the ratio :

$$\frac{\sigma_B}{\sigma_S} = \frac{\sigma_{pp \rightarrow Process \rightarrow \gamma lX}}{\sigma_{pp \rightarrow \gamma W \rightarrow \gamma lX}}$$

Process	$b\bar{b}\gamma$	$t\bar{t}\gamma$	$Z\gamma$	$\gamma + jet$	$W + jet$	$b\bar{b}$	$t\bar{t}$
σ_B/σ_S	42	0.20	0.04	10000	500	550000	30

Table 1: *Ratio between the cross-sections of the backgrounds and the cross-section of the signal ($|\eta_\gamma|$ and $|\eta_l| < 2.5$) (see text)*

Rejection factors against jets faking electrons and photons have been taken according to previous detailed simulations. For photons we will use R= 10000 [6] and for electrons R=10^5 [7]. The designation of 'jet' does not include b-quark jets which are studied separately.

4.1 Review of cuts used to reduce the background

The distribution of the kinematic variables of the signal are shown in figure 3.

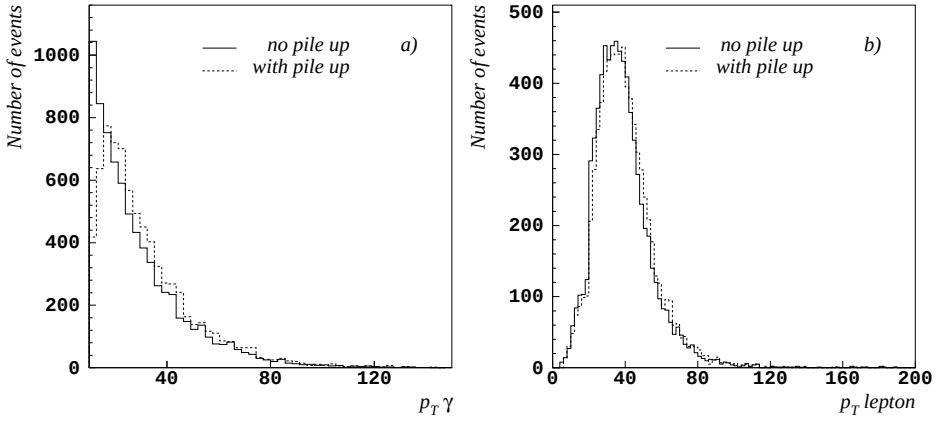


Figure 3: *Distribution of tranverse momentum of the photon (a) and the lepton (b) for the $W\gamma$ signal*

4.1.1 Selection using the photon

The minimum transverse momentum of the photon is chosen to be $p_{T_\gamma} > 100$ GeV. This cut corresponds to the kinematic domain of interest for the anomalous coupling study.

After applying the rejection factor jet/photon and jet/lepton as discussed above, the backgrounds corresponding to negligible cross-sections ($\sigma_B/\sigma_S < 1\%$) are eliminated.

We obtain then Table 2 for the relative importance of the backgrounds :

Process	$b\bar{b}\gamma$	$t\bar{t}\gamma$	$\gamma + jet$	$W + jet$	$b\bar{b}$	$t\bar{t}$
σ_B/σ_S	33	6	0.007	0.12	0.6	0.30

Table 2: *Ratio between the cross-sections of the backgrounds and of the signal, after applying the rejection against jets faking photons and electrons (see text)*

The same results are translated into numbers of expected events for one year of LHC running at design luminosity. Selection efficiencies of 90 % for the leptons and the photons are assumed.

Cut	$W\gamma$	$W + jet$	$b\bar{b}$	$t\bar{t}$	$b\bar{b}\gamma$	$t\bar{t}\gamma$
$p_{T_\gamma} > 100$ GeV	11500	1400	7000	3000	380000	75000

Table 3: *Signal and backgrounds, after cut on transverse momentum of photon, expected for one year of running at design luminosity.*

4.1.2 Selection using the lepton

To futher reduce the dominant $b\bar{b}\gamma$ background, we use the following isolation cut : the calorimeter transverse energy inside a cone of radius R=$\sqrt{\Delta\eta^2 + \Delta\phi^2}$=0.2, has to be below 12 GeV. This choice is justified by the distributions of the figures 4 and 5 where the isolation can be compared for a set of signal events ($W\gamma$) and a set of background events ($b\bar{b}$ and $t\bar{t}$), for no pile-up (figure 4) and including the expected pile-up at design luminosity (figure 5).

These figures show that the effect of pile-up on the efficiency of the isolation cut is important, but also that the rejection against electrons from $t\bar{t}$ is too small.

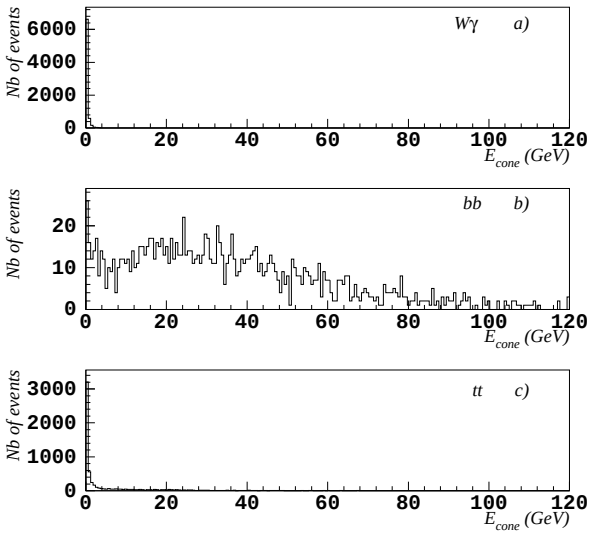


Figure 4: *Distribution of isolation variable for $W\gamma$ signal (a), for $b\bar{b}$ events (b) and for $t\bar{t}$ events (c) (no pile up)*

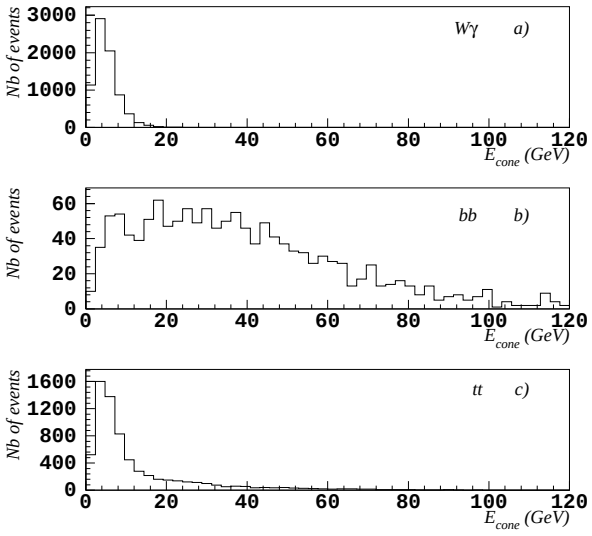


Figure 5: *Distribution of isolation variable for $W\gamma$ signal (a), for $b\bar{b}$ events (b) and for $t\bar{t}$ events (c) (with pile-up of 40 minimum biais)*

Finally it turns out that the transverse momentum of the lepton is strongly correlated to the photon momentum in the pair production of $W\gamma$ and so that, with $p_{T_\gamma} > 100$ GeV, a cut $p_{T_l} > 40$ GeV keeps a good $W\gamma$ efficiency and reduces considerably the $b\bar{b}$ and $b\bar{b}\gamma$ backgrounds.

The numbers corresponding to the three cut applied :

p_{T_γ}, p_{T_l} and isolation of lepton are shown in table 4 (for one year of LHC running).

Cut	$W\gamma$	$W + jet$	$b\bar{b}$	$t\bar{t}$	$b\bar{b}\gamma$	$t\bar{t}\gamma$
$p_{T_\gamma} > 100$ GeV + $p_{T_l} > 40$ GeV	9500	900	1100	1100	50000	13000
+ Isolation	9100	800	25	900	950	10500

Table 4: *Signal and backgrounds, after cuts on the transverse momenta of the photon and of the lepton, expected for one year of running at design luminosity. Also shown is the improvement expected from applying isolation cuts.*

4.2 Selection from "hadronic activity"

After all the previous cuts are applied, the remaining background events come mainly from $t\bar{t}\gamma$ process where a real $W\gamma$ pair can be produced in the decay chain. But in that case the difference with respect to the direct production of $W\gamma$ is a strong hadronic activity associated with the $W\gamma$ pair.

First we use any second isolated lepton that could come from the second W (with p_T above 10 GeV and $\eta < 2.5$) as a veto.

We have then to find a new variable that characterises this hadronic activity. We will use the transverse momentum of an extra jet in the event. If we use a cut on the most energetic (i.e. highest p_T, $|\eta| < 5$) extra jet in the events, asking for 85%

of efficiency : $p_{T\,extra\,jet} < 50$ GeV, we obtain a reduction factor of 0.14. The most energetic jet in $t\bar{t}\gamma$ events is mainly coming from the hadronic decay of one W, so there is another potentialy high p_T jet in the event. If we put a cut on the second most energetic extra jet , asking for 85% of efficiency : $p_{T\,second\,extra\,jet} < 25$ GeV, we gain a factor two in the rejection (reduction factor of 0.07).

The cut is fixed at $p_{T\,second\,extra\,jet} < 25$ GeV.

The effect of such a cut is shown in figure 6 for signal events and for $t\bar{t}\gamma$ events.

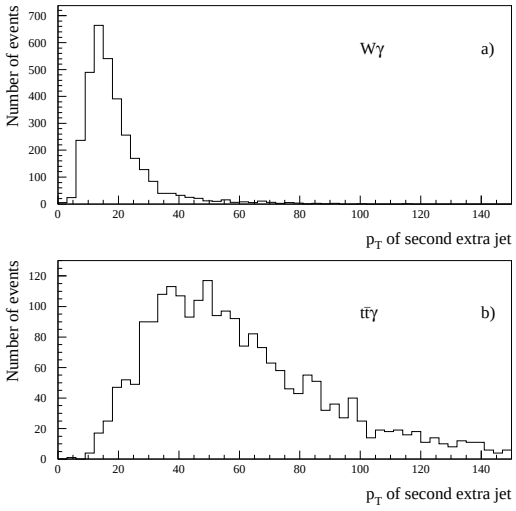


Figure 6: *Distribution of the transverse momentum of extra jet in the event for the signal (a) and for the $t\bar{t}\gamma$ events (b).*

4.3 Results after all cuts

Table 5 summarises the final set of cuts used and Table 6 summarises the results for the signal and background. We obtain 7500 $W\gamma$ pairs with 25% of background for one year of run at nominal high luminosity.

Cut
$\|\eta_\gamma\| < 2.5$
$\|\eta_l\| < 2.5$
$p_{T\,\gamma} > 100$ GeV
$p_{T\,l} > 40$ GeV
$E_{cone} < 12$ GeV (Isolation)
$p_{T\,second\,extra\,jet} < 25$ GeV

Table 5: *Cuts used to reduce the backgrounds to the $W\gamma$ signal*

Cut	$W\gamma$	$W+jet$	$b\bar{b}$	$t\bar{t}$	$b\bar{b}\gamma$	$t\bar{t}\gamma$
$p_{T\gamma} > 100$ GeV	11500	1400	7000	3000	380000	75000
$+\ p_{Tl} > 40$ GeV	9500	900	1100	1100	50000	13000
+ Isolation	9100	800	25	900	950	10500
$+\ p_{T\,second\,extra\,jet} < 25$ GeV	7500	650	14	90	40	750

Table 6: *Expected signal and backgrounds after all cuts, for one year of running at design luminosity.*

4.4 Sensitivity to κ_γ and λ_γ

Possible non-standard couplings lead to deviations from the Standard Model. Those deviations are the signals we will now search for in the various kinematic variables and their significance will be compared to the expected Standard Model plus backgrounds rates.

4.4.1 Signal of anomalous coupling

A dipolar form factor is used for the anomalous coupling, with a cut-off Λ equal to 10 TeV. This results in an effective coupling that does not violate unitarity [8].

We use the most sensitive variables to compare the Standard Model predictions to those from a model with an anomalous coupling :

a) the photon transverse momentum $p_{T\gamma}$.

b) the transverse mass M_T is computed following the definition given in [9] :

$$M_T^2 = (p_{T\nu} + \sqrt{(m_{l\gamma}^2 + p_{Tl\gamma}^2)})^2 - (p_{T\nu} + p_{Tl\gamma})^2$$

$$with \qquad p_{Tl\gamma} = p_{Tl} + p_{T\gamma} \qquad and \qquad m_{l\gamma}^2 = (\tilde{p_l} + \tilde{p_\gamma})^2$$

This definition allows to obtain a sharper jacobian peak when compared to a classical one.

c) to compute the photon rapidity it is necessary to be in the referential of the $W\gamma$ pair and so to know the W momentum. This momentum is computed using the W-mass constraint and we will therefore have two solutions for each event and use both with a weight of one half. The variable used is :

$$|y^*| = \left| \frac{1}{2}\, ln \frac{1+\cos\theta}{1-\cos\theta} \right|,$$

,

where θ is the angle between the photon and the beam direction in the $W\gamma$ pair reference system. A cut $p_{T\gamma} > 200$ GeV is used to enhance the sensitivity to a possible anomalous coupling.

Figures 7,8,9 for κ_γ and 10,11, 12 for λ_γ show the deviations of the expected distributions from the Standard Model predictions (including background) after all cuts.

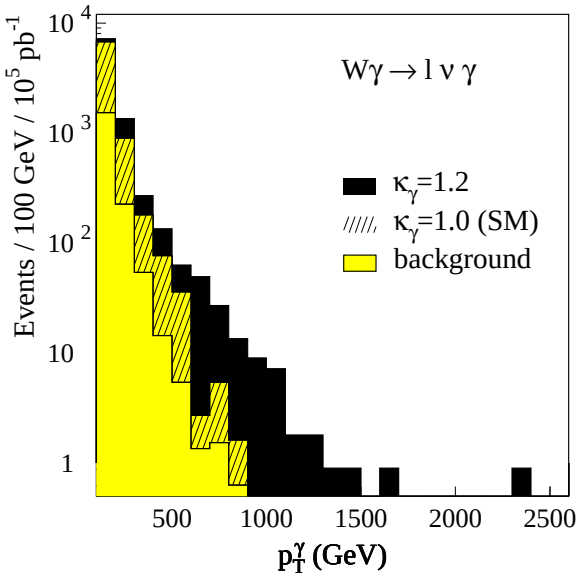


Figure 7: *Effect of anomalous coupling κ_γ on the distribution of the photon transverse momentum*

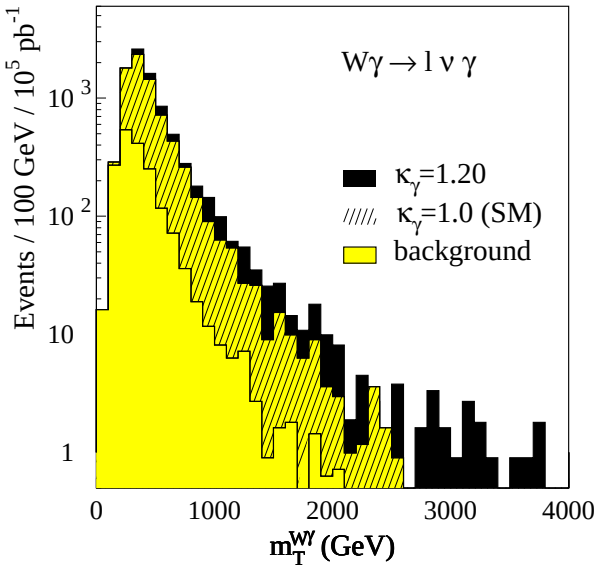


Figure 8: *Effect of anomalous coupling κ_γ on the distribution of the $W\gamma$ pair transverse mass*

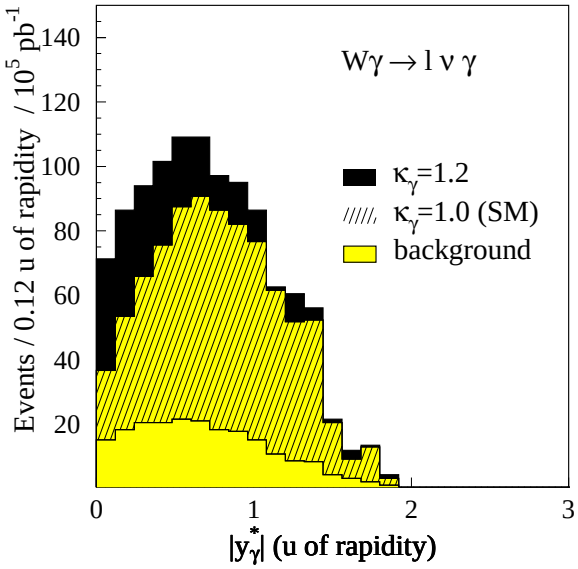


Figure 9: *Effect of anomalous coupling κ_γ on the distribution of the pseudo-rapidity of the photon, after the additional cut $p_{T\gamma} > 200\ GeV$*

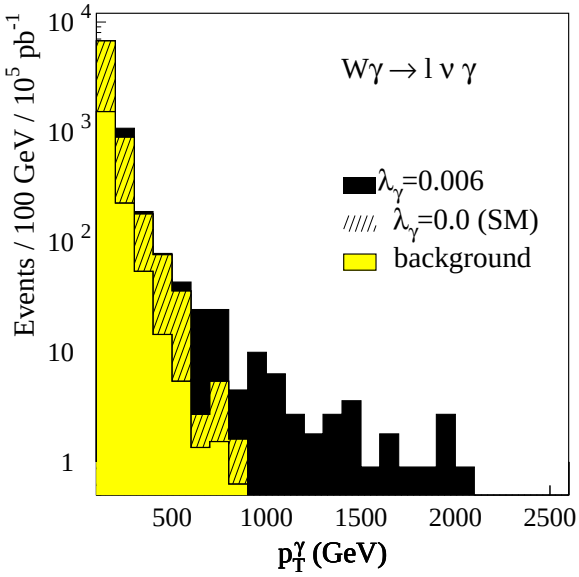


Figure 10: *Effect of anomalous coupling λ_γ on the distribution of photon transverse momentum*

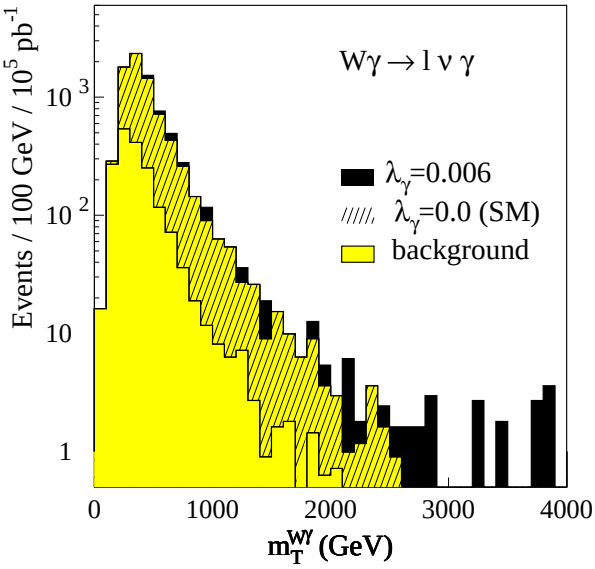


Figure 11: *Effect of anomalous coupling λ_γ on the distribution of the $W\gamma$ pair transverse mass*

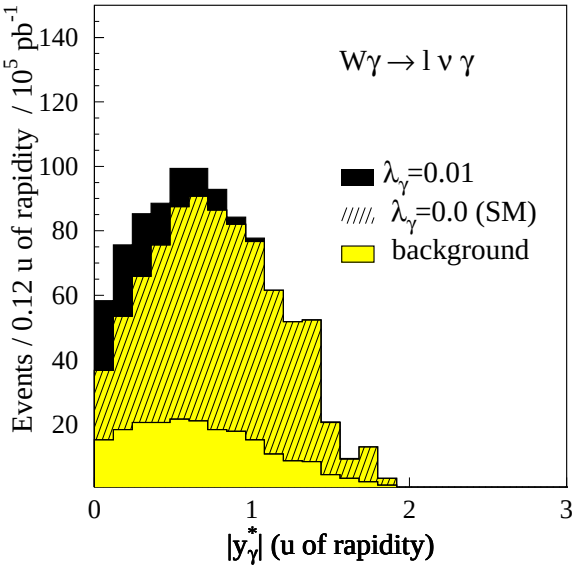


Figure 12: *Effect of anomalous coupling λ_γ on the distribution of the pseudo-rapidity of the photon, after the additional cut $p_{T\gamma} > 200\ GeV$*

4.4.2 Estimation of the sensitivity to anomalous couplings

We now wish to estimate the minimal change, with respect to the standard values of the parameters κ_γ and λ_γ, that would results in a significant deviation in the measured distributions. A significant deviation is defined as at least five standard deviations away from the Standard Model predictions.

We first restrict ourselves to the kinematic area where the deviation from the Standard Model is maximal. The boundaries of this region are obtained by requiring a total of at least fifteen events as expected by the Standard Model.

The cuts are then :

$p_{T\gamma} > 600$ GeV, $M_{TW\gamma} > 2000$ GeV and $|y^*| < 0.15$ (together with $p_{T\gamma} > 200$ GeV).

For each distribution, the five standard deviation limit in sensitivity is extracted. The results are given in tables 7 to 9, as well as the expected signal and background rates.

Parameter	Standard Model	B	Total measured	ΔS	$\Delta S/\sqrt{SM+B}$
$\kappa_\gamma = 1.11$	15.5	4.5	42	22	5.
$\lambda_\gamma = 0.0038$	15.5	4.5	42	22	5.

Table 7: *Event rates and sensitivity using the $p_{T\gamma}$ variable for 10^5 pb^{-1}.*

Parameter	Standard Model	B	Total measured	ΔS	$\Delta S/\sqrt{SM+B}$
$\kappa_\gamma = 1.19$	13	1	33	19	5.
$\lambda_\gamma = 0.0050$	13	1	32	18	4.8

Table 8: *Event rates and sensitivity using the $m_{TW\gamma}$ variable for 10^5 pb^{-1}.*

Parameter	Standard Model	B	Total measured	ΔS	$\Delta S/\sqrt{SM+B}$
$\kappa_\gamma = 1.18$	24.5	16.	72	32	5.
$\lambda_\gamma = 0.0110$	24.5	16.	72	32	5.

Table 9: *Event rates and sensitivity using the $|y^*|$ variable for 10^5 pb^{-1}.*

To estimate the incidence of the background on the measurement, we increased the background by a factor 10 and obtained new limits on the anomalous coupling parameters. The results are presented in tables 10 to 12.

Parameter	Standard Model	B	Total measured	ΔS	$\Delta S/\sqrt{SM+B}$
$\kappa_\gamma = 1.14$	15.5	44	96	37	4.8
$\lambda_\gamma = 0.005$	15.5	44	98	39	5.

Table 10: *Event rates and sensitivity using the $p_{T\gamma}$ variable with a factor 10 worse background for 10^5 pb^{-1}.*

Parameter	Standard Model	B	Total measured	ΔS	$\Delta S/\sqrt{SM+B}$
$\kappa_\gamma = 1.21$	13	10	47	24	5.
$\lambda_\gamma = 0.0055$	13	10	46	23	4.8

Table 11: *Event rates and sensitivity using the $m_{TW\gamma}$ variable with a factor 10 worse background for 10^5 pb^{-1}.*

Parameter	Standard Model	B	Total measured	ΔS	$\Delta S/\sqrt{SM+B}$
$\kappa_\gamma = 1.26$	23	140	218	61	4.8
$\lambda_\gamma = 0.0160$	23	140	218	61	4.8

Table 12: *Event rates and sensitivity using the $|y^*|$ variable with a factor 10 worse background for 10^5 pb^{-1}.*

In conclusion, if the background is multiplied by a factor 10, the sensitivity of course decreases but precision tests of possible anomalous couplings are still possible.

5 Study of WZ production

Restricting ourselves to the leptonic decays of W and Z we search for events containing three high p_T leptons. The backgrounds arise then from the following processes:

- Three real leptons:

  $pp \to Zb\bar{b}\ (+\ \mathrm{X}) \to lll\nu\ (+\mathrm{X})$
  $pp \to t\bar{t}\ (+\ \mathrm{X}) \to lll\nu\ (+\mathrm{X})$
  $pp \to b\bar{b}\ (+\ \mathrm{X}) \to lll\nu\ (+\mathrm{X})$

- two leptons plus one misidentified jet as an electron:

  $pp \to Z + jet\ (+\ \mathrm{X}) \to ll + jet\ (+\mathrm{X})$
  $pp \to t\bar{t}\ (+\ \mathrm{X}) \to ll + jet\ (+\mathrm{X})$
  $pp \to b\bar{b}\ (+\ \mathrm{X}) \to ll + jet\ (+\mathrm{X})$

In table 13, the ratio :

$$\frac{\sigma_B}{\sigma_S} = \frac{\sigma_{pp\to Process\to\gamma lX}}{\sigma_{pp\to\gamma W\to\gamma lX}},$$

is shown for the various background processes

Process	$Zb\bar{b}$	$b\bar{b}(lll)$	$t\bar{t}(lll)$	$Z + jet$	$b\bar{b}(ll + j)$	$t\bar{t}(ll + j)$
σ_B/σ_S	21	4 10^8	32000	55000	4.7 10^8	53000

Table 13: *Ratio of the backgrounds cross section to the WZ signal cross section*
In the following, we will assume that the e/jet ratio is equal to 10^5

5.1 Review of cuts used to reduce the background

The distribution of the kinematic variables of the signal are shown in figures 13 and 14.

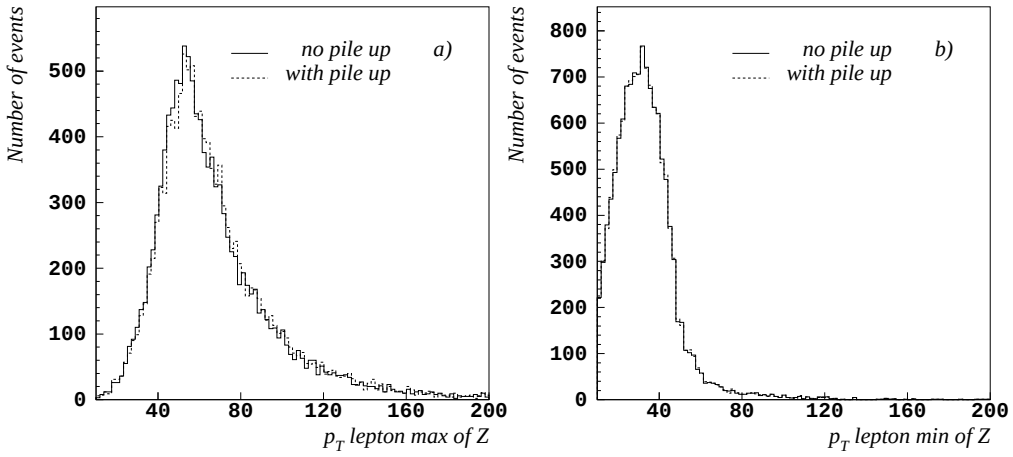


Figure 13: *Transverse momentum distributions of the two leptons associated to the Z from the WZ signal, for the one with higher (resp. lower) momentum in (a) (resp. (b)).*

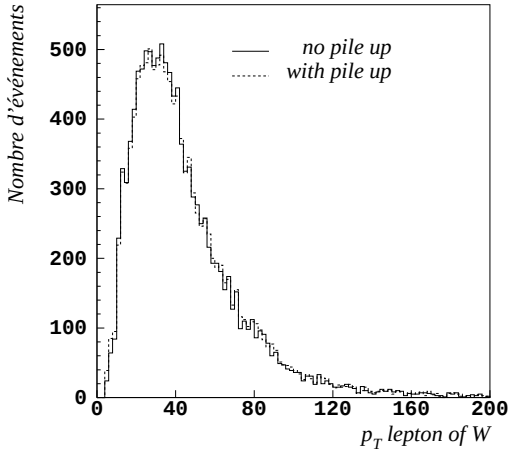


Figure 14: *Transverse momentum of the lepton associated to the W from the WZ signal*

First, a trigger on three leptons ($p_{T_{lepton}} > 10$ GeV) is required and we compute the invariant mass of all opposite charge pairs. The pair that minimizes $|M_{inv(ll)} - M_Z|$ is chosen to be the one coming from the Z decay. Then the W is reconstructed using the remaining lepton and the missing transverse momentum is identified with the neutrino transverse momentum.

5.1.1 Selection using the two leptons coming from the Z

The cut on the transverse momentum of the two leptons is in fact a cut on the smaller one. It is fixed at $p_{T_{lepton\ Z}} > 25$ GeV and suppresses the $b\bar{b}$ background

In order to reduce the $t\bar{t}$ background, a cut on the transverse mass of the pair is fixed at $|M_{invll} - M_Z| < 10$ Gev. (see figure 15)

This cut is very efficient to reduce $t\bar{t}$ background (see figure 15).

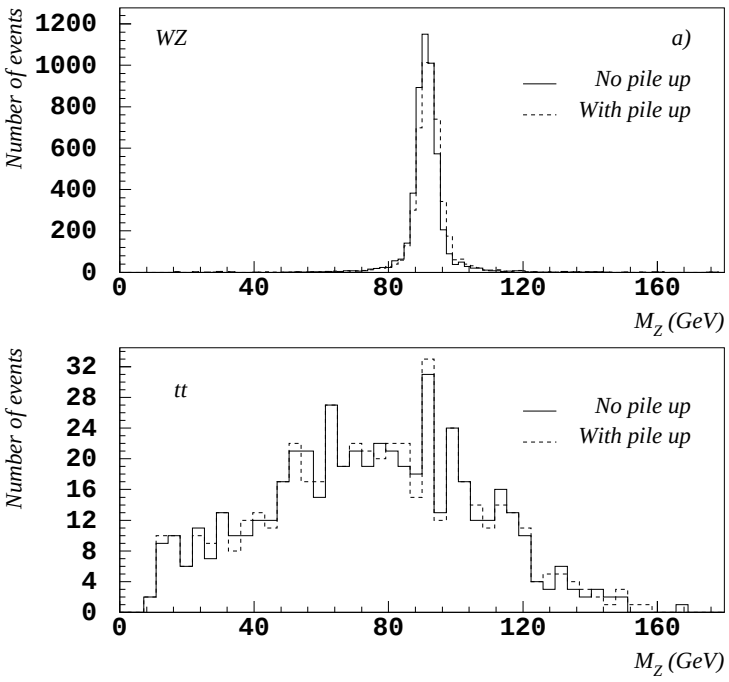


Figure 15: *Distribution of invariant mass of lepton pairs for a WZ signal (a) and for the $t\bar{t}$ background (b)*

After a cut $p_{T\,lepton\ Z} > 25$ GeV, $p_{T\,lepton\ W} > 10$ GeV, isolation $E_{cone} < 10$ GeV (the isolation cut has been chosen in order to have a good rejection of $t\bar{t}$ and $b\bar{b}$ background) and $|M_{invll} - M_Z| < 10$ Gev we obtain the results of table 14. The lepton efficiency was assumed to be 90% per lepton.

Cut	WZ	$t\bar{t}\ (lll)$	$Z + b$	$Z + jet$	$t\bar{t}\ (ll + j)$	$b\bar{b}\ (ll + j)$
$p_{T\,leptonZ} > 25$ GeV and $p_{T\,leptonW} > 10$ GeV	7700	350000	15000	1200	230	770
+ Isolation of the two leptons from Z	6500	140000	13000	1100	100	< 10
+ $\|M_{invll} - M_Z\| < 10$ Gev	6200	50000	12000	1100	17	< 10

Table 14: *Signal and backgrounds after a cut on the transverse momentum of the lepton from Z ; jet rejection factor = (1 per 100000)*

5.1.2 Selection using the lepton coming from the W

The cut on the transverse momentum of the lepton from W is fixed at $p_{T\,lepton\,W} >$ 25 GeV. This cut is efficient for reducing the $Zb\bar{b}$ and $t\bar{t}$ backgrounds with three real leptons.

We reconstruct the transverse invariant mass of the W with :

$$M_{T\,W}^{2} = 2p_{T\,l}p_{T\,\nu}(1 - cos\phi_{l\nu})$$

where $cos\phi_{l\nu}$ is the azimuthal angle between $p_{T\,l}$ and $p_{T\,\nu}$.

The cut is fixed at $M_{T\,W} > 40$ GeV (see figure 16)

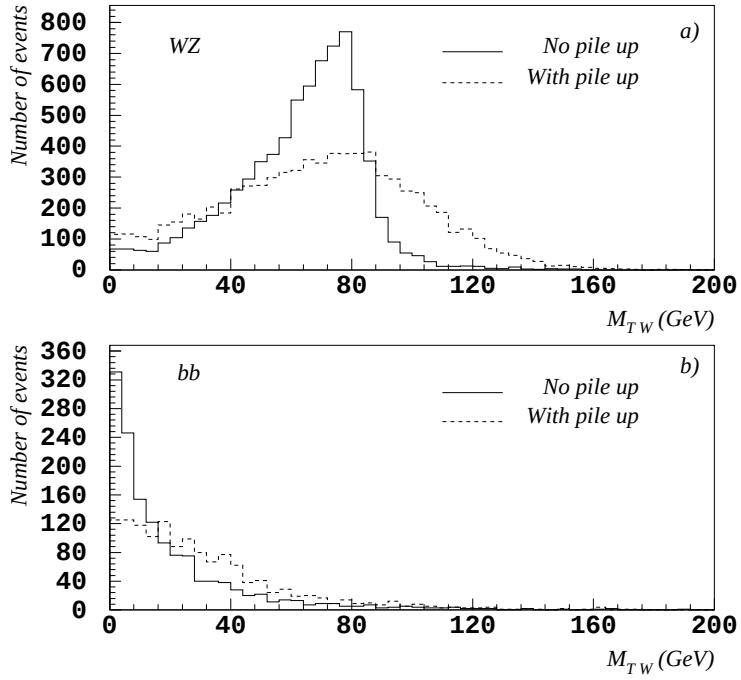


Figure 16: *Distribution of transverse invariant mass of lepton-neutrino pair for a WZ signal (a) and for the $b\bar{b}$ background (b)*

The results after all cuts (see table 15) are summarized in table 16.

Cut
$\|\eta_{leptons}\| < 2.5$
$p_{T\,leptons\,Z} > 25$ GeV
$p_{T\,lepton\,W} > 25$ GeV
$E_{cone} < 10$ GeV (Isolation)
$\|M_{invll} - M_Z\| < 10$ GeV
$M_T W > 40$ GeV

Table 15: *Cuts used to reduce the backgrounds to the WZ signal*

Cut	WZ	$t\bar{t}\ (lll)$	$Z+b$	$Z+jet$	$t\bar{t}\ (ll+j)$	$b\bar{b}\ (ll+j)$
Cut with Z and $p_{T\,lepton\,W} > 25$ GeV	4700	21000	4000	50	6	< 10
+ Isolation of lepton from W	4200	1050	100	50	6	< 10
+ $M_{TW} > 40$ GeV	3500	900	25	18	-	-

Table 16: *Expected signal and backgrounds after cuts on transverse momentum of Z and W leptons and on boson masses, for one year of running at design lumnosity.*

5.2 Sensitivity to κ_Z and λ_Z

5.2.1 Signal of anomalous coupling

We use the most sensitive variables to compare the Standard Model predictions to those from a model with an anomalous coupling :

a) the transverse momentum p_{TZ} is obtained with the two associated leptons.

b) the invariant mass of the pair WZ is defined by :

$$M_{TWZ}^2 = (p_{T\nu} + \sqrt{(m_{lZ}^2 + p_{TlZ}^2)})^2 - (p_{T\nu} + p_{TlZ})^2$$

$$where \quad p_{TlZ} = p_{Tl} + p_{TZ} \qquad and \qquad m_{lZ}^2 = (p_l^\mu + p_Z^\mu)^2$$

Figures 17,18 for κ_Z and 19 20 for λ_Z show the deviations of the expected distributions from the Standard Model predictions (including background) after all cuts.

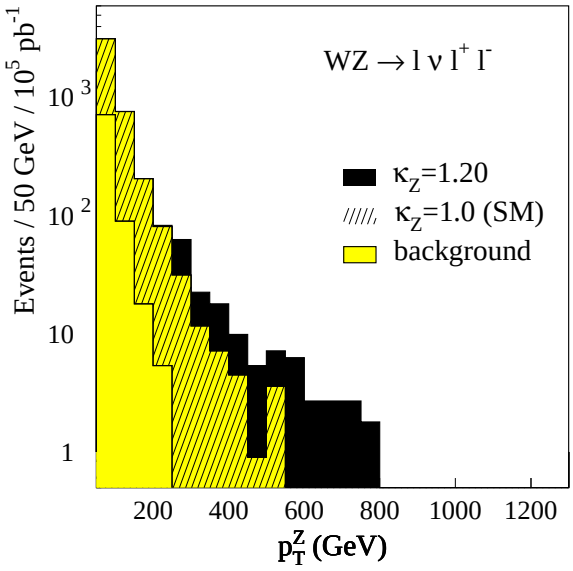


Figure 17: *Effect of anomalous coupling κ_Z on the distribution of the Z transverse momentum*

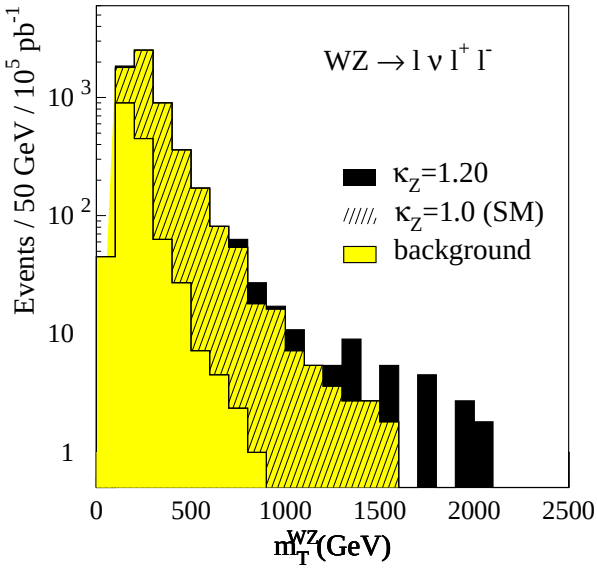


Figure 18: *Effect of anomalous coupling κ_Z on the distribution of the WZ pair transverse mass*

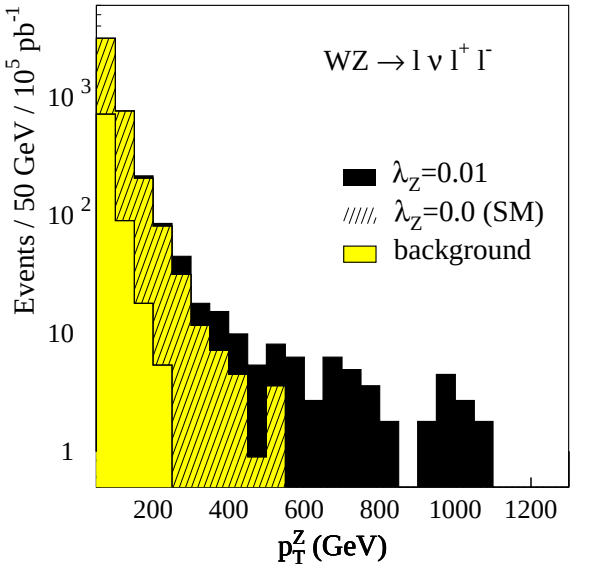


Figure 19: *Effect of anomalous coupling λ_Z on the distribution of the Z transverse momentum*

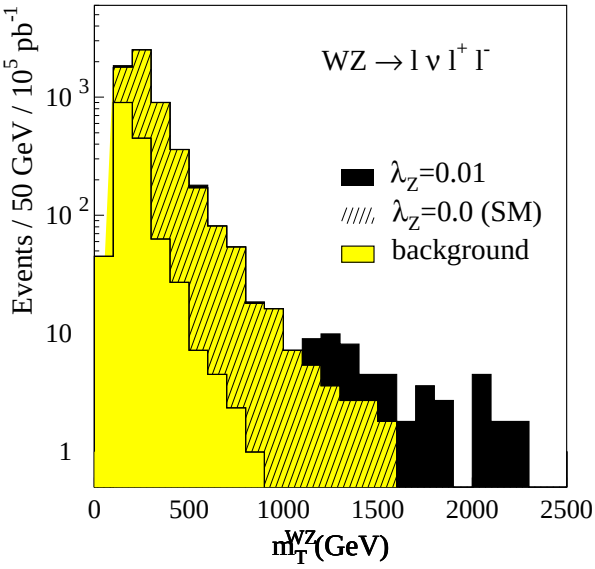


Figure 20: *Effect of anomalous coupling λ_Z on the distribution of the WZ pair transverse mass*

5.2.2 Estimation of the sensitivity to anomalous couplings

The methods and definitions are identical to what has been described for the $W\gamma$ case.

The cuts are then : $p_{TZ} > 380$ GeV, $M_{TWZ} > 1000$ GeV.

The results are given in tables 17 and 18, as well as the expected signal and background rates.

Parameter	Standard Model	B	Total measured	ΔS	$\Delta S/\sqrt{SM+B}$
$\kappa_Z = 1.20$	15.5	0.4	36	20	5.
$\lambda_Z = 0.01$	15.5	0.4	36	20	5.

Table 17: *Events rates and sensitivity using the p_{TZ} variable for 10^5 pb^{-1}.*

Parameter	Standard Model	B	Total measured	ΔS	$\Delta S/\sqrt{SM+B}$
$\kappa_Z = 1.22$	24	0.5	49	24.5	5.
$\lambda_Z = 0.01$	24	0.5	49	24.5	5.

Table 18: *Events rates and sensitivity using the m_{TWZ} variable for 10^5 pb^{-1}.*

6 Conclusion

The results obtain for both $W\gamma$ and WZ production study shows that the ATLAS detector as the capability to detect anomalous coupling in the three boson vertices or to push the limits of theses anomalies up to less than 1% of accuracy for the most sensibles parameters.

$\lvert\kappa_\gamma - 1\rvert < 0.11$
$\lvert\lambda_\gamma\rvert < 0.004$
$\lvert\kappa_Z - 1\rvert < 0.20$
$\lvert\lambda_Z\rvert < 0.01$

Table 19: *Sensitivity at 5 standard deviation to anomalous coupling*

References

[1] R. Casalbuoni, S. De Curtis, D. Dominici and R. Gatto, Phys. Lett **B155** (1985) 95; Nucl. Phys. **B282** (1987) 235.

[2] T.G. Rizzo Phys. Rev. **D32** (1985) 43.

[3] G.J. Gounaris, F.M. Renard, Z. Phys. **C 59** (1993) 133-141.

[4] M.D. Scadron, Advanced quantum theory, Springer-Verlag (1979).

[5] *ATLAS, Letter of Intent for a General-Purpose pp Experiment at the Large Hadron Collider at CERN*, CERN/LHCC/92-4 (1992)

[6] L. Fayard and G. Unal, EAGLE note, INDET-NO-001 (1992)

[7] A.G. Clark *et al.*, ASCOT/EAGLE note,INDET-NO-015 (1992)
P. Nevski *et al.*, ATLAS note, INDET-NO-017 (1992)

[8] U. Baur and D. Zeppenfeld, Nucl. Phys. **B308** (1988) 127.

[9] Barger, Phys. Lett. 125 B (83) 339